

New Theoretical Approach to Nuclear Heavy-Ion Scattering*

KEITH A. BRUECKNER, J. ROBERT BUCHLER, AND MICHAEL M. KELLY

Department of Physics and Institute for Pure and Applied Physical Sciences, University of California, San Diego, La Jolla, California 92037

(Received 15 January 1968)

A new theoretical approach to the study of the nuclear interaction between heavy ions is presented. The potential governing the collision between complex nuclei is derived from a statistical theory of finite nuclei based on nuclear-matter calculations and is presented as an application to the O^{16} - O^{16} elastic scattering process. A phase-shift analysis of the experimental data on O^{16} - O^{16} scattering is performed which shows, first, that an excellent fit can be obtained with a real potential up to 14 MeV, and second, that there exists a short-range repulsion. The best-fit potential is in close agreement with the calculated potential in the attractive region, but has a weaker and shorter-range repulsion.

I. INTRODUCTION

IN the last few years, investigations of heavy-ion scattering have received considerable attention. Improvements in beam techniques have renewed the interest in scattering problems between complex nuclei.^{1,2} Theoretical analyses using standard phenomenological optical potentials have provided, up to now, reasonable fits to some of the experimental data.³ In contrast to the usual processes in which the projectile is either a single particle or consists of a very small number of nucleons, there is no *a priori* justification to assume a Saxon-Woods-type well for the nuclear potential in the case of heavy ions.

A general treatment of the collision between heavy ions would require the solution of the Hartree-Fock-type equations for the system projectile-target in each point of the trajectory. The complexity of the many-body problem involved here can, however, be greatly reduced by replacing the Hartree-Fock method by a statistical approach. It is the purpose of the present paper to show how this treatment can be achieved in the framework of a statistical theory of finite nuclei based on nuclear-matter calculations. The method we are proposing is quite general and can be applied to various reactions between complex nuclei. As an application we present the O^{16} - O^{16} elastic scattering whose unusual features are of particular interest.

In Sec. II, the derivation of the scattering potential is given in some detail together with the application to O^{16} . In Sec. III, the phase-shift analysis is discussed, showing that it is possible to fit the existing experimental

data on O^{16} - O^{16} elastic scattering (i.e., the 13-MeV angular distribution and the 90° excitation function up to 14 MeV) with a purely real potential and that there is strong evidence for the existence of a short-range repulsion. Conclusions are presented in Sec. IV.

II. DERIVATION OF THE ELASTIC SCATTERING POTENTIAL

The energy of a fermion system in its ground state can be expressed as a functional of the density which is stationary with respect to variations of the density.⁴ In the spirit of the Thomas-Fermi model, we introduce the local density approximation which consists of assuming that the relation between volume energy and density is locally the same as in nuclear matter. This allows us to derive the potential energy of the many-nucleon system from the saturation curve of nuclear matter as obtained by Brueckner, Coon, and Dabrowski⁵ by a *K*-matrix calculation. Variations of the density, especially at the surface of the nucleus where the effect of the finite range of the nuclear forces is important, are taken into account by means of density gradient corrections. Assuming that the proton and neutron densities are proportional to each other in light nuclei, we express the energy per unit volume in the form

$$\mathcal{E}(\rho(r)) = \left\{ \kappa_{\text{kin}} \rho(r)^{5/3} + \rho(r) V(\rho(r)) + C_{\text{kin}} \frac{(\nabla \rho(r))^2}{\rho(r)} + C_{\text{pot}} (\nabla \rho(r))^2 + \frac{1}{2} e \rho(r) \Phi_c(r; \rho) \right\}, \quad (1)$$

where

$$\kappa_{\text{kin}} = 0.3 \left(\frac{3}{2} \pi^2 \right)^{3/2} \hbar^2 / M \quad \text{and} \quad C_{\text{kin}} = \hbar^2 / 72M. \quad (2)$$

The origin of Eq. (1) has been discussed in detail in Ref. 6. The first two terms represent the kinetic and the potential energy. The third term is the purely kinematical gradient correction due to exchange, whereas the fourth

⁴ P. Hohenberg and W. Kohn, Phys. Rev. **136**, B864 (1964).

⁵ Keith A. Brueckner, S. Coon, and J. Dabrowski, Phys. Rev. (to be published); referred to as B. C. D.

⁶ K. A. Brueckner, J. R. Buchler, S. Jorna, and R. J. Lombard (unpublished).

* This research was supported in part by the U.S. Atomic Energy Commission.

¹ (a) D. A. Bromley, J. A. Kuehner, and E. Almqvist, Phys. Rev. **123**, 878 (1961); (b) R. H. Siemssen, J. V. Maher, A. Weidinger, and D. A. Bromley, Phys. Rev. Letters **19**, 369 (1967); (c) D. A. Bromley, contribution to the Enrico Fermi Summer School on Nuclear Structure and Nuclear Reactions, Varenna, 1967 (unpublished).

² E. B. Carter, P. H. Stelson, M. K. Mehta, and D. L. Bernard, Nucl. Phys. **63**, 575 (1964).

³ See, e.g., R. H. Bassel, G. R. Satchler, and R. M. Drisko, Nucl. Phys. **89**, 419 (1966); J. A. Kuehner and E. Almqvist, in *Proceedings of the Third Conference on Reactions between Complex Nuclei, Asilomar, 1963*, edited by A. Ghiorso *et al.* (University of California Press, Berkeley, 1963), where other references are given.

term results from the long-range part of the nuclear forces. The last term is the Coulomb energy. The only phenomenological parameter C_{pot} is adjusted so as to give the experimental binding energy for O^{16} and Ca^{40} .⁶

Minimization of the total energy of the system

$$E[\rho] = \int (dr)^3 \mathcal{E}(\rho(r)) \quad (3)$$

with respect to the density was achieved by varying several three-parameter trial functions. The results are in close agreement with those obtained by solving the Lagrange-type differential equation associated with (3). The ground-state densities are found to be of the form

$$\rho(r) = \rho_0(1 + pr^2 + tr^3) \{1 + \exp[(r^2 - R^2)/B^2]\}^{-1}. \quad (4)$$

In the case of O^{16} , the optimum set of parameters are $R = 2.7$ fm, $B = 1.555$ fm, $p = 0$, and $t = -0.009$ fm⁻³ leading to a binding energy of 125.25 MeV, a central density of 0.193 fm⁻³, a radius of 2.54 fm, and a surface thickness of 2.14 fm. The region ($r > t^{-1/3}$), where this density is set equal to zero, falls well outside the "surface" region so that this unphysical cut-off has negligible effects. The validity of this conclusion was checked by fitting an exponential tail to the density at 10% of its central value.

The extension of the statistical theory to a system of two interacting nuclei is straightforward. In fact, the interaction energy $W(R)$, as a function of the distance between the centers of the colliding nuclei, is very simply given by the total energy of the system at the separation distance R minus the total energy of the separated systems, i.e.,

$$\begin{aligned} W(R) &= E[\rho_1 + \rho_2] - E[\rho_1] - E[\rho_2] \\ &\equiv \int (dr)^3 \{ \mathcal{E}[\rho(|\mathbf{r} + \frac{1}{2}\mathbf{R}|)] + \mathcal{E}[\rho(|\mathbf{r} - \frac{1}{2}\mathbf{R}|)] \\ &\quad - \mathcal{E}[\rho(|\mathbf{r} + \frac{1}{2}\mathbf{R}|)] - \mathcal{E}[\rho(|\mathbf{r} - \frac{1}{2}\mathbf{R}|)] \}. \quad (5) \end{aligned}$$

We now assume that the energy functional is given by our statistical approximation (1) and that the density function $\rho(r)$ is the optimal ground-state function (4) as obtained by the minimization of (1). We have thus assumed that the densities of the interacting nuclei superimpose adiabatically without distortion during the collision so that the total energy of the system is still expressed by the same energy functional (3). A justification of the assumption of adiabaticity lies in the fact that the kinetic energy of the nucleons inside the nucleus (≈ 42 MeV) is much larger than the kinetic energy associated with their relative motion during the collision (≈ 1 MeV). The omission of polarization effects in the elastic range may be justified by the large excitation energy of the 3⁻ state in O^{16} (6.13 MeV), which prevents easy distortion during the collision.

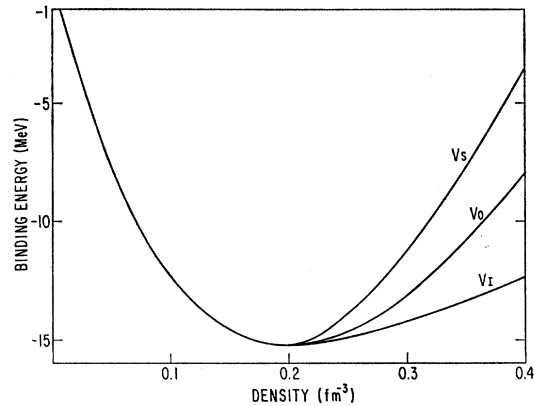


Fig. 1. Nuclear-matter saturation curves. The curve V_0 has been obtained by B. C. D.; the curves V_I and V_S have been chosen to test the high-density behavior on the O^{16} - O^{16} interaction potential.

We expect the interaction potential to be very sensitive to the high-density behavior of the saturation curve, since the total density becomes larger than the normal density of nuclear matter. The K -matrix formalism, however, is based on a low-density expansion, so that it loses reliability at high densities. For these reasons we have examined the effect of departures from the computed high-density saturation curve. Three potentials W_0 , W_I , and W_S are given in Fig. 1; the first one corresponds to the saturation curve of Brueckner *et al.*,⁵ whereas the other two result from the curves having a lower and a higher slope, respectively.

We have plotted the "nuclear" part of the resulting potentials, i.e., omitting the Coulomb interaction, for the three different saturation curves in Fig. 2. It can be seen that the height of the short-range repulsion is strongly influenced by the saturation curve of nuclear

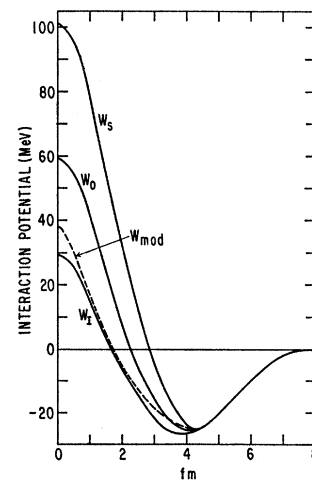


Fig. 2. Nuclear part of the elastic scattering potential. The potential W_0 is obtained from B. C. D.'s nuclear matter calculations, whereas W_S and W_I come from the saturation curves labeled V_S and V_I , respectively (cf. Fig. 1). W_{mod} is the best-fit potential.

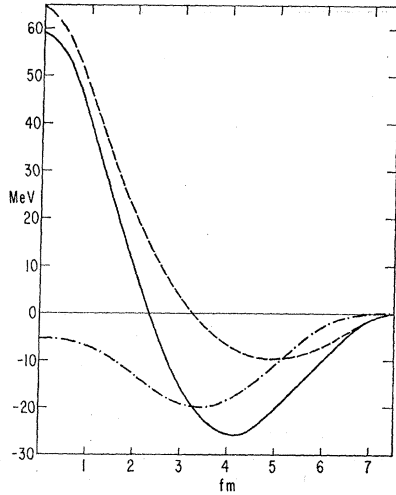


FIG. 3. Contributions to the interaction potential W_0 (solid line) from the homogeneous term (dash-dot line) and from the density gradient correction (dash line).

matter at high density. Figure 3 shows separately the contributions to the "nuclear" potential stemming from the "volume" term and from the inhomogeneity correction. The short-range repulsion is seen to come about through the combination of the saturation effects in nuclear matter and of the increase in inhomogeneity.

The addition of the Coulomb interaction, calculated with the density distribution (4), yields a nonmonotonic potential with a dip of about 17 MeV, exhibited in Fig. 4. The height of the Coulomb barrier, as determined by the range of the nuclear potential, is in good agreement with the energy at which the experimental excitation function deviates from its Mott value.

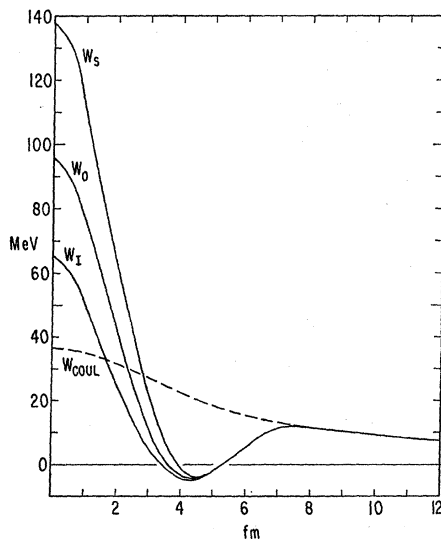


FIG. 4. Total scattering potential (including exact Coulomb interaction).

Although there are many reactions with a negative Q value (the S^{32} ground state, e.g., has a Q of -16.54 with respect to the O^{16} - O^{16} system at rest), the large density rearrangement required for these processes implies a very small transition probability. On the other hand, the Ne^{20} - C^{12} reaction channel (α -particle exchange), e.g., or the excitation of the collective (vibrational) 3^- state of O^{16} , which have a much larger overlap with the elastic channel, have a Q of 2.43 and 6.13 MeV, respectively. These reactions are excited only if sufficient kinetic energy is available as the nuclei reach nuclear interaction range. This justifies the use of a real potential up to energies of about 14 MeV. The phase-shift analysis confirms this assumption, as will be shown in the next section.

III. PHASE-SHIFT ANALYSIS

In this section, we shall first indicate the possibility of fitting the experimental data with a real potential, show the existence of a short-range repulsion, and then check the predictions of the three calculated potentials with experiment.

In the case of two potentials, one of which is short-ranged, we have the well-known⁷ relation between the phase-shift and the differential cross section:

$$\frac{d\sigma}{d\Omega} = |f(\theta) + f(\pi - \theta)|^2, \quad (6)$$

with

$$f(\theta) = f_{\text{Coul}}(\theta) + \frac{1}{2ik} \sum (2l+1) e^{2i\sigma_l} (e^{2i\eta} - 1) P_l(\cos\theta). \quad (7)$$

The Coulomb scattering amplitude $f_{\text{Coul}}(\theta)$ and phase shifts σ_l are given by

$$f_{\text{Coul}}(\theta) = \frac{-\gamma}{2k \sin^2(\frac{1}{2}\theta)} \exp\{-i\gamma \ln \sin^2(\frac{1}{2}\theta) + 2i\sigma_0\}, \quad (8)$$

and

$$\sigma_0 = \arg\Gamma(1+i\gamma) = -0.5772\gamma + \sum_{\zeta=1}^{\infty} \frac{\gamma}{\zeta} \tan^{-1}\left(\frac{\gamma}{\zeta}\right), \quad (9)$$

$$\sigma_l = \arg\Gamma(l+1+i\gamma) = \sigma_0 + \sum_{\zeta=1}^l \tan^{-1}\left(\frac{\gamma}{\zeta}\right), \quad (10)$$

with

$$\gamma = (Ze)^2/\hbar v.$$

With the help of these relations we have carried out a χ^2 search to fit the experimental data using an unweighted χ^2 , defined as

$$\chi^2 = \sum_i \frac{(O_i - C_i)^2}{\Delta_i^2},$$

⁷ See, e.g., L. Schiff, *Quantum Mechanics* (McGraw-Hill Publishing Co., New York, 1956).

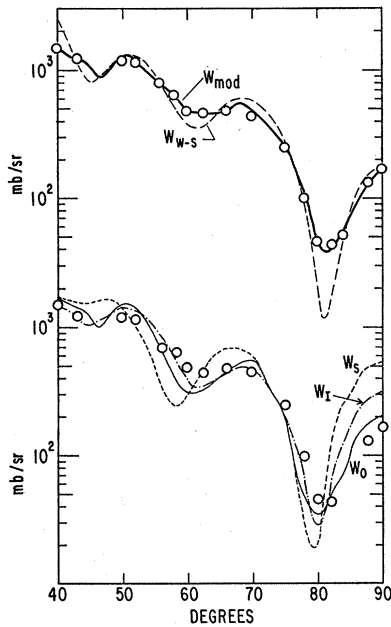


FIG. 5. 13-MeV (c.m.) angular distribution. The lower three curves have been obtained from the potentials W_s , W_0 , and W_I . The upper curves correspond to the modified potential (solid line) and the best-fit Saxon-Woods potential (dashed). The circles are the experimental data.

where O_i is the experimental value, C_i is the calculated value, and Δ_i is the probable error of the measurement. In our analysis, we have estimated the measurement errors from the plots of Ref. 1a because of the unavailability of more precise data. The errors used in the analysis are shown in Fig. 5 and 6.

From the height of the Coulomb plus nuclear barrier, it may be easily shown that only the first four phase shifts, namely, η_0 , η_2 , η_4 , and η_6 , could be significantly different from zero at 13 MeV, which was confirmed later by an actual calculation (Fig. 7). Thus, we could limit our search to four parameters, which yielded a unique set of real phase shifts given in Table I. The χ^2 for the 15 data points from 50° – 90° was less than 11 (i.e., the number of independent data). The deviations in the inferred experimental phase shifts given in Table I represent the range of values which may be varied simultaneously to yield a χ^2 fit less than 11. By varying one or more of these phase shifts to at least 1°

TABLE I. 13-MeV phase shifts (in deg).

Phase shifts	Inferred experimental values	W_{W-S}^a	W_0	W_I	W_S
η_0	355 ± 5	353	344	342	340
η_2	312 ± 7	342	286	277	258
η_4	150 ± 10	273	104	138	180
η_6	52 ± 15	79	50	74	110

^a Best Woods-Saxon potential.

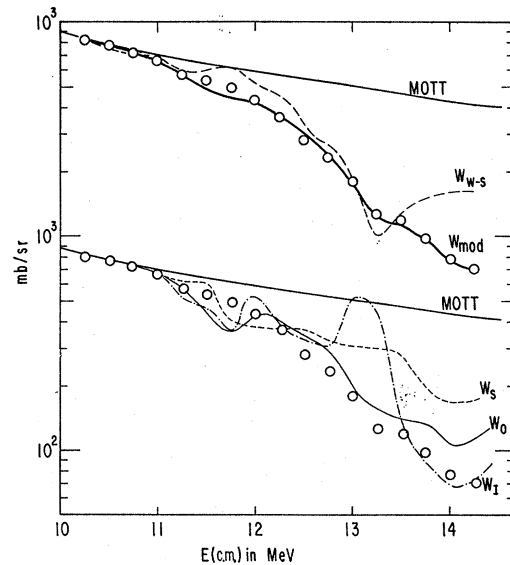


FIG. 6. 90° excitation function. The lower three curves have been calculated with the potentials W_s , W_0 , and W_I . The upper curves represent the fit to the experimental data (circles) obtained from the modified potential (solid line) and the best-fit Saxon-Woods potential (dashed).

outside of the given range yields a minimum χ^2 of 14.2 which is a comparatively poor fit. Thus we may conclude that a real potential with range and barrier height close to the predicted values is sufficient to give an excellent fit to the data.

At very low energy, the deviation from Mott scattering is negligible since the probability of particle penetration into the range of the nuclear interaction is very small. Thus, for such energies, all the η_i 's are zero. As the energy increases, the various partial waves start to

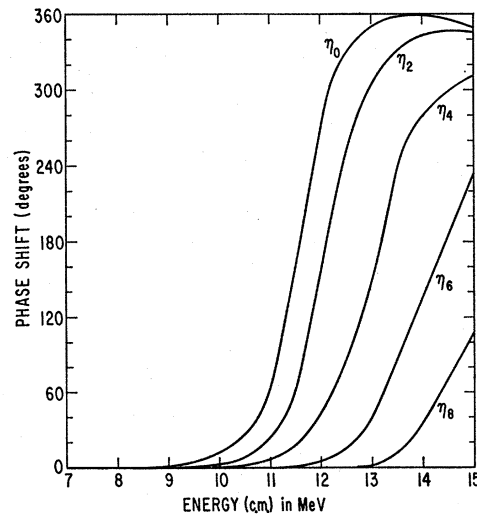


FIG. 7. First five phase shifts as a function of energy (calculated from the potential W_0).

experience the nuclear interaction successively and their phase shifts increase. For a nonmonotonic potential each η_l increases very slowly as a function of energy until barrier transmission starts to occur. As the barrier is passed, the η 's rapidly reach their maximum value and they decrease slowly with increasing energy. This behavior is exhibited in Fig. 7, confirming the assumption that only four nuclear phase shifts are needed at 13 MeV.

We have also calculated the 90° excitation function as a further test of the predicted potentials. The $l=8$ nuclear phase shift has been included, giving a small contribution at the higher energies.

In Fig. 5, we have plotted the 13-MeV angular distribution corresponding to the three calculated potentials W_0 , W_I , and W_S , and Fig. 6 shows the 90° excitation functions. The χ^2 's for these potentials are 23.5, 24.2, and 25.7, respectively, for the 13-MeV angular distribution. The excitation function for W_0 is close to experiment, while the predictions for W_I and W_S show large excursions from the measured values.

To improve the fit to the data and to see which of the details of the potential, i.e., the range, the well depth, or the height and width of the repulsion, governs the scattering, we have parametrized the potential. The comparison of the calculated angular distribution and 90° excitation function with the experimental one allows us then to determine the appropriate parameters of the potential. Because the WKB approximation provides a close relationship between potential and phase shifts, we first calculated the η 's in this approximation. However, the WKB phase shifts have proved to be a poor approximation to the exact phase shifts for energies near the barrier. Nevertheless, they provide a useful guide in indicating the direction and magnitude of the required changes in the potential parameters.

It is found that a small modification of the parameters of the potential W_0 , namely, an increase in range of 0.24 fm, a decrease in the attractive well depth of 0.6 MeV, and a reduction of 0.7 fm of the "core" radius is sufficient to reproduce the best phenomenological phase shifts at 13 MeV (see Table I) and to fit the 90° excitation function up to 14 MeV. The modified potential is given in Fig. 2. This reduction of the "core" radius may result from a change in the saturation curve at high density or from a decrease in the effect of gradient corrections for the superimposed nuclear densities. The other smaller differences between the best-fit potential and the calculated potential W_0 may be caused by the breakdown of the statistical formula (3) at small densities or from polarization corrections.

To investigate further the possibility of a fit with a potential of simpler form, we attempted to obtain a fit to the angular distribution with a Saxon-Woods potential. This yielded a χ^2 of 23 for the optimal set of parameters $\{V_0=-23.1$ MeV, range = 7.2 fm, and diffuseness = 1.1 fm}. An attempt to make the excita-

tion function fall off from Mott at the correct energy by increasing the radius increases the χ^2 to 26.3. Thus the evidence for a short-range repulsion is quite strong.

Finally, we should point out that we were unable to fit the excitation function beyond 14 MeV with a real potential, probably because of the onset of inelastic scattering.

IV. CONCLUSIONS

We have shown that in the $O^{16}-O^{16}$ scattering, a good fit can be obtained over a narrow energy range with a real potential. A short-range repulsion, as predicted by a statistical treatment of nuclear saturation, is also confirmed in some detail. The calculated potential, resulting from the rather delicate balance between the saturation effects of nuclear forces and the inhomogeneity corrections resulting from the density rearrangement, differs somewhat in the range and strength of the short-ranged repulsion from the modified potential which has been determined to meet the very stringent test of fitting both the differential cross section at 13 MeV and the 90° excitation function up to 14 MeV. The impossibility of obtaining a fit to the excitation function at higher energies with real phase shifts reflects the opening of reaction channels, probably the $Ne^{20}-C^{12}$ channel, as well as of inelastic channels. A preliminary complex-phase-shift analysis above 14 MeV indicates that once the partial waves have passed the Coulomb barrier and penetrate into the "core" region, they acquire very rapidly a substantial imaginary part. Hence the absorptive part of the potential is expected to depend strongly on energy and angular momentum. Recently, Block⁸ has done an extensive investigation with real potentials and, although reproducing successfully the main features of the excitation function (i.e., the four broad peaks), he finds a cross section two orders of magnitude too large, which confirms our conclusion that strong absorption occurs at energies higher than 14 MeV. For these reasons, the study of $O^{16}-O^{16}$ scattering is of great interest near the reaction thresholds where relatively simple models may still be used successfully. At higher energies, when the "core" has become black, many exit channels will be open and the elastic channel will be occupied with a probability proportional to its statistical weight and available phase space. An investigation of these reaction thresholds is being completed and will be the subject of a subsequent paper.

As pointed out before, our method is not confined to O^{16} elastic scattering, but can be extended to the other light nuclei like C^{12} , Ne^{20} , or Ca^{40} . The treatment of heavier nuclei (Ce^{140} , Pb^{208}), however, requires a slight modification in the energy functional (1), to take care of the nonproportionality of the proton and neutron densities. The analysis of the scattering of light nuclei (e.g., C^{12} , Ne^{20}), which are not as rigid as O^{16} or Ca^{40} ,

⁸ B. Block (to be published, private communication).

is doubly complicated through the existence of low-lying collective excitations. Absorption sets in at a lower energy so that the range, where a purely real potential can be used, is more restricted. Polarization effects, resulting from the virtual transitions to the collective excited states, can no longer be ignored, since they may considerably alter the range and strength of the real potential. Nevertheless a potential like (5) is still ex-

pected to be a good starting point for the study of these nuclei.

ACKNOWLEDGMENTS

It is a pleasure to thank Dr. B. Block and especially Dr. R. J. Lombard for valuable discussions. One of us (J.R.B.) gratefully acknowledges a research grant by the Luxembourg Ministère des Affaires Culturelles.

Search for the Ground State of ${}^5\text{H}$ by means of the ${}^3\text{H}(t,p)$ Reaction*

P. G. YOUNG, RICHARD H. STOKES, AND GERALD G. OHLSEN

Los Alamos Scientific Laboratory, University of California, Los Alamos, New Mexico 87544

(Received 22 April 1968)

Proton spectra from the ${}^3\text{H}(t,p){}^5\text{H}$ and ${}^3\text{He}(t,p){}^5\text{He}$ reactions have been measured with a triton bombarding energy of 22.25 MeV. Narrow $T=\frac{3}{2}$ states in the $A=5$ system were not observed in either reaction. However, in the ${}^3\text{H}(t,p)$ reaction broad peaks appeared in the proton spectra at energies consistent with a ${}^5\text{H}$ state 1.8 MeV above the $t+2n$ mass. The possibility that this peak can be attributed to the ground state of ${}^5\text{H}$ is discussed.

THE possible existence of a particle-stable ${}^5\text{H}$ nucleus has been the subject of a number of papers.¹ Theoretical estimates for the mass of the ground state of ${}^5\text{H}$ range from a suggestion that ${}^5\text{H}$ is particle-stable by 0.6 MeV² to predictions that the ground state is unstable by several MeV.³ Most experimental attempts to observe ${}^5\text{H}$ have been sensitive only to a bound ${}^5\text{H}$ system. For example, searches for β^- or delayed neutron activity from the ${}^7\text{Li}(p,3p){}^5\text{H}$, ${}^3\text{H}(t,p){}^5\text{H}$, and ${}^7\text{Li}(\pi^-,pn){}^5\text{H}$ reactions have yielded negative results.¹ Although one report of β^- activity from the ${}^7\text{Li}(\gamma,2p){}^5\text{H}$ reaction has been made,⁴ negative results were obtained when the experiment was repeated under only slightly different conditions.⁵ The few previous experiments which permitted detection of unbound ${}^5\text{H}$ states provide only negative results. For instance, no evidence for narrow states in ${}^5\text{H}$ (bound or unbound) was found in a recent study of ${}^9\text{B}$ spectra from the ${}^9\text{Be}(\alpha,{}^9\text{B}){}^5\text{H}$ reaction.⁶ In another recent experiment a search was made for the ground state of ${}^5\text{Be}$ using the ${}^3\text{He}({}^3\text{He},n){}^5\text{Be}$ reaction.⁷ The results

indicate that ${}^5\text{Be}$ lies at least 4.2 MeV above the ${}^3\text{He}+2p$ mass, which suggests that ${}^5\text{H}$ is unbound by at least 2.1 MeV.

A firm limit on the stability of ${}^5\text{H}$ can be obtained from the fact that the ground state of ${}^9\text{Li}$ is stable with respect to heavy-particle emission. That is, ${}^5\text{H}$ cannot be bound by more than 8.55 MeV or ${}^9\text{Li}$ would be unstable to ${}^5\text{H}+{}^4\text{He}$ decay. In a recent study of the ${}^3\text{H}(d,p){}^4\text{H}$ and ${}^3\text{H}(t,d){}^4\text{H}$ reactions, Jarmie *et al.* report no evidence for a bound ${}^4\text{H}$ nucleus in the energy range 0–12.8 MeV below the $n+t$ mass.⁸ Assuming then that ${}^4\text{H}$ is unbound and using the systematics of neutron pairing energies,⁹ a less certain estimate of 2.9 MeV for the maximum binding energy of ${}^5\text{H}$ can be obtained.¹⁰

To form a state in ${}^5\text{H}$ in the vicinity of the $t+2n$ mass with the ${}^3\text{H}(t,p){}^5\text{H}$ reaction, a triton beam energy of at least 17 MeV is required. In the present experiment a tritium-filled gas target was bombarded with 22.25-MeV tritons from the Los Alamos three-stage electrostatic accelerator, and the energy spectra of protons were observed at four angles. The detection system consisted of a ΔE gas proportional counter followed by a 1000- μm fully depleted surface-barrier E detector. The effective thickness of the proportional-counter gas was equivalent to 21 μm of Si. A second solid-state detector located immediately behind the E detector was used to reject protons which had sufficient energy (>12 MeV) to penetrate the E detector. After satisfying a coincidence requirement, the E and ΔE energy spectra were

* Work performed under the auspices of the U. S. Atomic Energy Commission.

¹ T. Lauritsen and F. Ajzenberg-Selove, Nucl. Phys. **78**, 1 (1966); for a review of ${}^5\text{H}$, see A. I. Baz, V. I. Goldanskii, and Ya. B. Zeldovich, Usp. Fiz. Nauk **85**, 455 (1965) [English transl.: Soviet Phys.—Usp. **8**, 177 (1965)].

² C. H. Blanchard and R. G. Winter, Phys. Rev. **107**, 774 (1957).

³ R. F. Fraser and B. M. Spicer, Australian J. Phys. **19**, 893 (1966).

⁴ B. M. K. Nefkens, Phys. Rev. Letters **10**, 55 (1963).

⁵ N. K. Sherman and P. Barreau, Phys. Letters **9**, 151 (1964).

⁶ R. L. McGrath, J. Cerny, and S. W. Cosper, Phys. Rev. **165**, 1126 (1968).

⁷ E. G. Adelberger, A. B. McDonald, T. A. Tombrello, F. S. Dietrich, and A. V. Nero, Phys. Letters **25B**, 595 (1967).

⁸ N. Jarmie, R. H. Stokes, G. G. Ohlsen, and R. W. Newsome, Jr., Phys. Rev. **161**, 1050 (1967).

⁹ V. I. Goldanskii, Zh. Eksperim. i Teor. Fiz. **38**, 1637 (1960) [English transl.: Soviet Phys.—JETP **11**, 1179 (1960)].

¹⁰ In this calculation, the neutron pairing energy of ${}^5\text{H}$ is assumed to be less than that of ${}^5\text{He}$ (2.9 MeV).